Electronic Supplementary Material (ESI) for ChemComm.

Supporting Information

Novel Aza-BODIPY based Small Molecular NIR-II Fluorophores for *in vivo* Imaging

Lei Bai,[a,†] Pengfei Sun,[b,†] Yi Liu,[a,†] Hang Zhang,[a] Wenbo Hu,[a] Wansu Zhang,[b] Zhipeng Liu,[a,*] Quli Fan,[b,*] Lin Li[a,*] and Wei Huang[a,b,c]

[a]*Key Laboratory of Flexible Electronics (KLOFE) & Institute of Advanced Materials (IAM), Nanjing Tech University (NanjingTech), Nanjing 211816, China.* iamlli@njtech.edu.cn; iamzpliu@njtech.edu.cn

[b]*Key Laboratory for Organic Electronics and Information Displays & Institute of Advanced Materials (IAM), Nanjing University of Posts & Telecommunications, Nanjing 210023, China.* iamqlfan@njupt.edu.cn.

[c]*Shaanxi Institute of Flexible Electronics (SIFE), Northwestern Polytechnical University, 127 West Youyi Road, Xi'an 710072, China*

1. Materials and characterization

All the chemical reagents were purchased from Aldrich or TCI. Commercially available reagents were used without further purification. *N*, *N*-Dimethylformamide (DMF), 1, 2-dichloroethane (DCE) and dichloromethane (CH_2Cl_2, DCM) were distilled over CaH_2. Petroleum ether (PE, 60~90°C), DCM, Ethyl acetate (EA) and Methanol (MeOH) were used as eluents for Flash column chromatography with Merck silica gel (0.040-0.063). Reaction progress was monitored by TLC on pre-coated silica plates (250 μm thickness) and spots were visualized by ceric ammonium molybdate, basic $KMnO_4$, UV light or iodine. Reaction progress was monitored by TLC on pre-coated silica plates (250 μM thickness) and spots were visualized by UV light or iodine. All reactions were carried out under a dry nitrogen protection. Silica gel 60 (200-300 mesh, Silicycle) was used for column chromatography. All reagents and solvents were purchased from commercial suppliers and used without further purification. ^1H and ^{13}C NMR spectra were collected in $CDCl_3$ or DMSO-d_6 at 25°C using an Avance AV-300 spectrometer. ^1H NMR coupling constants (J) are reported in Hertz (Hz) and multiplicity is indicated as follows: s (singlet), d (doublet), t (triplet), q (quartet), m (multiplet), dd (doublet of doublet). Mass spectra were recorded on a Finnigan LCQ mass spectrometer, a Shimadzu LC-IT-TOF spectrometer.

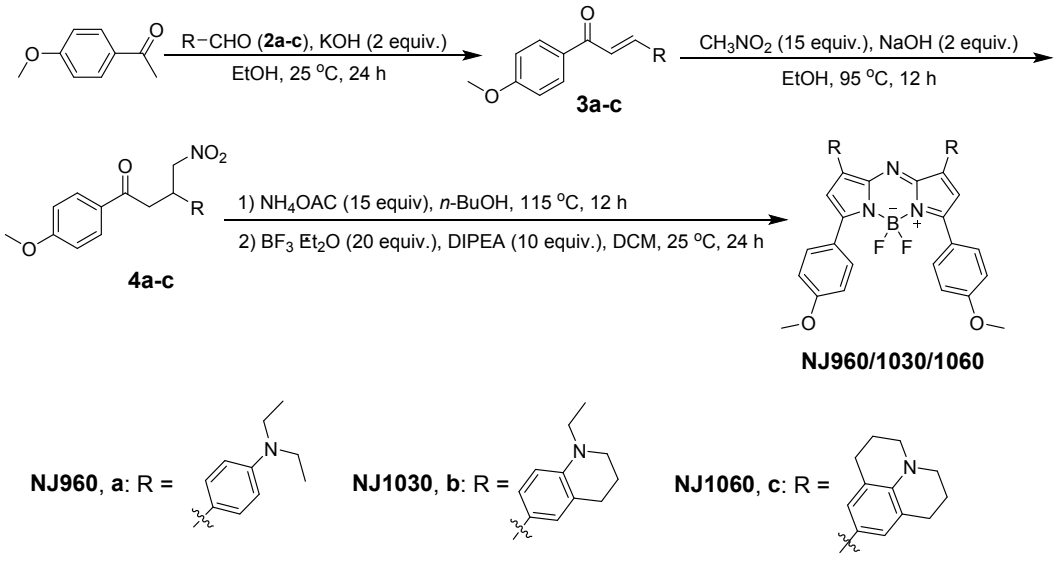

Scheme S1. The synthesis of **NJ960**, **NJ1030** and **NJ1060**.

2. Synthesis and characterization:

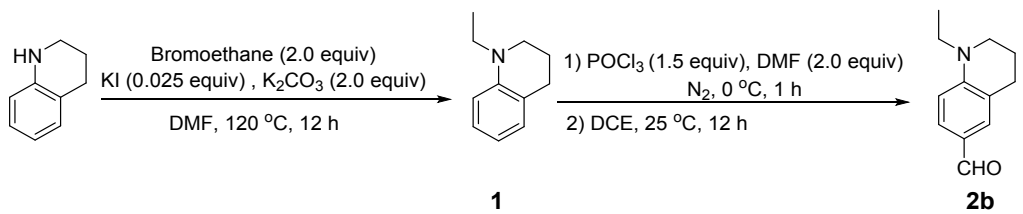

1 **2b**

Synthesis of **2b**: Under a N_2 atmosphere, anhydrous potassium carbonate (276.42 mg, 2 mmol) and potassium iodide (415 mg, 0.025 mmol) were added to a solution of 1,2,3,4-tetrahydroquinoline (133.2 mg, 30 mmol) and C_2H_5Br (217 mg, 2 mmol, 0.149 mL) in DMF (20 mL). The mixture was stirred at 120 °C for 12 h, and then poured into water and organic phase was extracted by EA, The combined organic fractions were dried over anhydrous Na_2SO_4, filtered and concentrated to afford the crude residue which was purified *via* flash chromatography on a silica column (10 : 1 v/v PE: EA) to afford the compound as a yellow oil (**1**, yield: 85%). ^{1}H NMR ($CDCl_3$) δ/ppm 7.06 (m, 1H), 6.95 (m, 1H), 6.60 (m, 2H), 3.33 (m, 4H), 2.77 (t, *J* = 6.0, 2H), 1.89 (m, 2H), 1.12 (t, *J* = 7.5, 3H). Then, DMF (0.93 mL, 12.4 mmol, 2.0 equiv.) was added to freshly distilled $POCl_3$ (1.42 g, 9.3 mmol,1.5 equiv.) under an atmosphere of N_2 at 0 °C and the mixture was stirred at room temperature for 1 h. After the addition of **1** (1.0 g, 6.2 mmol) in DCE (10 mL) dropwise, the mixture was stirred at room temperature overnight, then poured into a saturation aqueous solution of $NaHCO_3$. After 2 h stirring at room temperature, the mixture was extracted with EA, and the organic fractions were collected and dried over anhydrous Na_2SO_4. The crude product was purified by silica gel chromatography eluting with (PE : EA =10 : 1) to afford a yellow oil. (80% yield). ^{1}H NMR ($CDCl_3$) δ/ppm 9.64 (s, 1H), 7.52 (d, *J* = 9.0, 1H), 7.44 (s, 1H), 6.60 (d, *J* = 9.0, 1H), 3.38 (m, 4H), 2.77 (t, *J* = 6.0, 2H), 1.93 (m, 2H), 1.21 (t, *J* = 7.5, 3H).

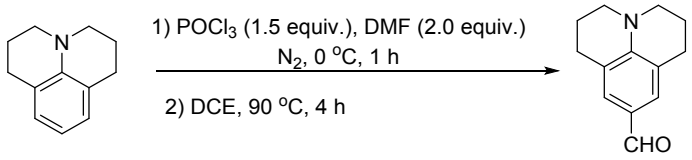

2c

Synthesis of **2c**: The compound was synthesized according to the similar procedure described above in **2b** by using julolidine to afford **2c** (yield: 90%) as a light yellow solid. ^{1}H NMR (300 MHz, $CDCl_3$) δ/ppm 9.59 (s, 1H), 7.28 (s, 2H), 3.28 (t, *J* = 6.0, 4H), 2.76 (t, *J* =6.0, 4H), 1.95 (m, 4H).

Synthesis of compound **3a-c**: A solution of **2a-c** (1.0 equiv., **2a** is commercial available compound), *p*-acetylanisole (1.0 equiv.), in EtOH (60 mL) was treated with NaOH (20% w/w in H_2O, 15 mL) and stirred at room temperature for 24 h. MeOH was removed under reduced pressure and the resultant aqueous solution was diluted with brine and extracted with EA. The combined organic fractions were dried over anhydrous Na_2SO_4, filtered and concentrated to afford the crude residue which was purified via flash chromatography on a silica column (15 : 1 v/v PE : EA) to afford the compounds as red solid.

3a (yield: 81%): ^{1}H NMR (300 MHz, $CDCl_3$) δ/ppm 8.01 (d, *J* = 9.0 Hz, 2H), 7.75 (d, *J* = 15.0 Hz, 1H), 7.54 (d, *J* = 9.0 Hz, 2H), 7.35 (d, *J* = 15.0 Hz, 1H), 6.98 (d, *J* =9.0 Hz, 2H), 6.67 (d, *J* =9.0 Hz, 2H), 3.88 (s, 3H), 3.42 (dd, J_1 = 15.0 Hz, J_2 = 9.0 Hz, 4H), 1.20 (t, *J* = 6.0 Hz, 6H).^{13}C NMR (75 MHz, $CDCl_3$) δ/ppm

188.97, 162.94, 149.60, 145.06, 132.06, 130.61, 122.11, 116.19, 113.68, 111.34, 55.37, 44.52,12.48.

3b (yield: 90%):^{1}H NMR (300 MHz, $CDCl_3$) δ/ppm 8.03 (d, *J* = 9.0 Hz, 2H), 7.76 (d, *J* = 15.0 Hz, 1H), 7.33 (m, 3H), 6.98 (d, *J* = 6.0 Hz, 2H), 6.58 (d, *J* = 9.0 Hz, 1H), 3.87 (s, 3H), 3.37 (m, 4H), 2.77 (t, *J* = 6.0 Hz, 2H), 1.96 (m, 2H), 1.17 (t, *J* = 6.0, 3H).^{13}C NMR (75 MHz, CDCl3) δ/ppm 188.93, 162.90, 147.29, 145.29, 132.35, 130.50, 129.44, 122.31, 122.14, 115.88, 113.66, 110.07,55.45, 48.64, 45.44, 28.15, 21.93, 11.12.

3c (yield: 80%): ^{1}H NMR (300 MHz, $CDCl_3$) δ/ppm 8.01 (d, *J* = 9.0 Hz, 2H), 7.73 (d, *J* = 15.0 Hz, 1H), 7.31 (d, *J* = 8.0 Hz, 1H), 7.11 (s, 2H), 6.98 (d, *J* = 6.0 Hz, 2H), 3.88 (s, 3H), 3.25 (t, *J* = 4.5 Hz, 4H), 2.79 (t, *J* = 6.0 Hz, 4H), 1.97 (m, 4H). ^{13}C NMR (75 MHz, $CDCl_3$) δ/ppm 188.87, 162.86, 145.48, 145.13, 132.20, 130.73, 130.48, 128.04, 121.91, 121.05, 115.67, 114.05,113.64, 55.45, 50.00, 27.74, 21.66.

Synthesis of compounds **4a-c**: To a stirred solution of **3a-c** (1.0 equiv.) in EtOH (10 mL) was added $MeNO_2$ (15 equiv.) and NaOH (20% w/w in H_2O, 80.0 µL). The reaction was refluxed for 24 h. EtOH was removed with reduced pressure and the resultant aqueous solution was diluted with brine (20 mL) and extracted with EA. The combined organic fractions were anhydrous Na_2SO_4, filtered and concentrated to afford the crude residue which was purified *via* flash chromatography on a silica column (10 : 1 v/v PE : EA) to afford the title compounds as tan oil.

4a (yield: 60%): ^{1}H NMR (300 MHz, $CDCl_3$) δ/ppm 7.89 (d, *J* = 9.0 Hz, 2H), 7.10 (d, *J* = 9.0 Hz, 2H), 6.93 (d, *J* = 9.0 Hz, 2H), 6.62 (d, *J* = 9.0 Hz, 2H), 4.77 (m, 1H), 4.63 (m, 1H), 4.08 (m, 1H), 3.88 (s, 3H), 3,66 (m, 8H),1.13 (t, *J* = 7.5 Hz, 6H). ^{13}C NMR (75 MHz, $CDCl_3$) δ/ppm 195.91, 163.76, 147.35, 130.39, 129.78, 128.29, 125.45 113.86, 112.02, 80.13, 55.51, 44.29, 41.57, 38.78.

4b (yield: 65%): ^{1}H NMR (300 MHz, $CDCl_3$) δ/ppm 7.89 (d, *J* = 9.0 Hz, 2H), 6.90 (m, 4H), 6.49 (d, *J* = 15.0 Hz, 1H), 4.76 (m, 1H), 4.60 (m, 1H), 4.03 (m, 1H), 3.86 (s, 3H), 3.28 (m, 6H), 2.70 (t, *J* = 6.0, 2H), 1.92 (m, 2H), 1.11(t, *J* = 7.5, 3H). ^{13}C NMR (75 MHz, $CDCl_3$) δ/ppm 196.04, 163.76, 139.86, 130.43, 124.74, 121.84, 113.87, 80.13, 58.51, 55.54, 49.91, 41.67, 38.85, 30.38, 27.71, 22.02, 18.40.

4c (yield: 60%): ^{1}H NMR (300 MHz, $CDCl_3$) δ/ppm 7.92 (d, *J* = 9.0 Hz, 2H), 6.93 (d, *J* = 9.0 Hz, 2H), 6.64 (s, 2H), 4,74 (m, 1H), 4.59 (m,1H), 1.93 (m, 4H). ^{13}C NMR (75 MHz, $CDCl_3$) δ/ppm 195.82, 163.76, 139.86, 130.43, 125.85, 121.84, 114.69, 113.87, 80.13, 58.51, 55.54, 49,96, 41.67, 38.85, 27.71, 22.02.

Synthesis of **NJ960**: A solution of **4a** (1.0 equiv.) was dissolved in *n*-butanol (20 mL). Ammonium acetate (15.0 equiv.) was added and the reaction was stirred at 115 °C for 12 h. The reaction was cooled to room temperature and the solvent was concentrated to 5 mL and filtered, and the isolated solid washed

with ethanol (2× 5 mL) to afford the title compound as a dark blue film. And the solution of dark blue film (1.0 equiv.) in anhydrous DCM (15 mL) was treated with anhydrous DIPEA (10.0 equiv.) and boron trifluoride etherate (15.0 equiv.), and stirred at room temperature under N_2 for 24 h. The solution was diluted with water (20 mL) and extracted with DCM. The combined organic fractions were dried anhydrous Na_2SO_4, filtered and concentrated to afford the crude residue which was purified via flash chromatography on a silica column (1 : 1 v/v PE : DCM) to afford **NJ960** as a metallic brown solid (yield: 90%). ^{1}H NMR (300 MHz, $CDCl_3$) δ/ppm 8.06 (t, J = 7.5 Hz, 8H), 7.00 (d, J = 9.0 Hz, 6H), 6.75 (d, J = 11.5 Hz, 6H), 3.87 (s, 6H), 3.47 (dd, J_1 = 15.0 Hz, J_2 = 6.0 Hz, 8H), 1.24 (t, J = 7.5 Hz, 12H). ^{13}C NMR (75 MHz, $CDCl_3$) δ/ppm 161.2, 156.7, 148.4, 145.2,145.0, 131.1, 125.2, 120.6, 114.3, 114.0, 111.4, 55.3, 44.6, 12.7. HRMS calcd for $C_{42}H_{45}BF_2N_5O_2$ $[M+H]^+$: 700.3634; found: 700.3662.

Synthesis of **NJ1030**: The compound was synthesized according to the similar procedure described above in **NJ960** by using **4b** to afford **NJ1030** (yield: 90%) as a metallic brown solid. ^{1}H NMR (300 MHz, $CDCl_3$) δ/ppm 8.0 (m, 6H), 7.79 (s, 2H), 6.98 (d, J = 15.0 Hz, 4H), 6.77 (t, J = 9.0, 6H), 5.30 (s, 1H), 3.86 (s, 6H), 3.65 (m, 1H), 3.42 (s, 7H), 3.10 (m, 1H), 2.84 (s, 3H), 2.02 (m, 4H), 1.22 (t, J = 7.5, 6H). ^{13}C NMR (75 MHz, $CDCl_3$) δ/ppm 161.1, 156.5, 147.2, 145.7, 145.2, 142.7, 131.1, 130.2, 129.4, 125.2, 122.7, 114.3, 113.9, 110.9, 55.3, 48.8, 45.9, 28.2, 21.9, 11.2. HRMS calcd for $C_{44}H_{45}BF_2N_5O_2$ $[M+H]^+$: 724.3634; found: 724.3623.

Synthesis of **NJ1060**: The compound was synthesized according to the similar procedure described above in **NJ960** by using **4c** to afford **NJ1060** (yield: 90%) as a metallic brown solid. ^{1}H NMR (300 MHz, $CDCl_3$) δ/ppm 8.02 (d, J = 12.0 Hz, 4H), 7.59 (s, 6H), 6.97 (d, J = 12.0 Hz, 4H), 6.72 (s, 2H), 3.86 (s, 6H), 3.27 (s, 4H), 2.77 (m, 4H), 2.01 (m, 4H). ^{13}C NMR (75 MHz，$CDCl_3$) δ/ppm 161.2, 156.7, 148.4, 145.2, 145.0, 131.1, 125.2, 120.6, 114.3, 114.0, 111.4, 55.3, 44.6, 12.7. HRMS calcd for $C_{46}H_{45}BF_2N_5O_2$ $[M+H]^+$: 748.3634; found: 748.3635.

3. Theoretical calculations

All the calculations were based on density functional theory (DFT) with B3LYP functional and 6-31G(d) basis set. Solvent (water) was considered in all the calculations. The UV-vis absorptions of the compounds (vertical excitation) were calculated with the TDDFT methods based on the optimized ground state geometry (S_0 state). For the fluorescence emission, the emission wavelength was calculated based on the optimized excited states (S_1 state). All these calculations were performed with Gaussian 09W.

4. Spectral characterization

Absorption spectra were recorded using SynergyHTX microplate reader. Emission spectra were recorded using an Edinburgh FLSP920 fluorescence spectrophotometer equipped with a picosecond pulsed semiconductor light (EPL375) and a microsecond flash-lamp (UF900). TEM images were taken on a JEOL-2100F at an acceleration voltage of 200 kV.

5. Measuring quantum yield.

The quantum yield of the probe was determined according the formula:

$$\Phi_x = \Phi_{st}(\frac{S_X}{S_{st}})(\frac{A_{st}}{A_X})(\frac{n^2{}_X}{n^2{}_{st}})$$

to where Φ_{st} is the quantum yield of the standard, S is the area under the emission spectra, A is the absorbance at the excitation wavelength, and n is the refractive index of the solvent used. x subscript denotes unknown, and st means standard. **IR26** (Φ_f = 0.1 in DCM) was chosen as the standard.

6. Photostability

The photo-stability of **NJ960**, **NJ1030**, **NJ1060** and **IR1061** (Sigma-Aldrich, CAS: 155614-01-0) were investigated in PBS solution containing 20% DMSO as co-solvent with concentration of 10 μM, The respective dye's solution in 1cm quartz cuvettes (200 μL) was illuminated with a continuous laser (808 nm, 100 mW/cm^2) for 60 min. the emission intensity of **NJ960**, **NJ1030**, **NJ1060** and **IR1061** was measured every 1 min.

7. The preparation of NJ1060 NPS

NJ1060 was be made to Water-soluble Nanoparticles (NPs) with Pluronic F-127 for *in vivo* imaging. **NJ1060** (2 mg) were dissolved in THF (1 mL) by bath sonication. Then, a mixed THF solution (1 mL) and Pluronic F-127 (10 mg/mL) were used to prepare **NJ1060** NPs by rapidly injecting the mixture into distilled-deionized water (9 mL) under continuous sonication with a microtip-equipped probe sonicator for 2 min. After sonication, THF was evaporated at room temperature. The aqueous solution washed three times using a centrifugal filter under centrifugation at 1500 rpm for 30 min. The concentration of **NJ1060** NPs solutions were determined by UV-Vis absorption according to their absorption coefficients.

8. Chicken penetration model assay (NJ1060 NPs)

NJ1060 NPs (0.1 mg/mL) was filled in a plastic hose (length: 2 cm, diameter: 2 mm). Then, the plastic hose was put on the surface of prepared

nuggets and taken for imaging. The deepths of penetration was tested through changing the different thickness (0, 1, 2, 4, 6, 8 and 10 mm) of chicken meat and detecting the varied fluorescence intensity of **NJ1060** NPs in the hose.

9. Cell culture and cytotoxicity activity assay

HepG2 cells were cultured in Dulbecco's Modified Eagle's Medium (DMEM), containing 10% FBS, 100.0 mg/L streptomycin, and 100 IU/mL penicillin. HepG2 cells were seeded in glass-bottom dishes (Mattek) and grown to 70-80% con-fluency. The cytotoxicity activities of the probes were determined using an XTT colorimetric cell proliferation kit (Roche), following the manufacturer guidelines. Briefly, cells were grown to 20-30% confluency (they would reach 80-90% confluency within 48-72 h in the absence of compounds) in 96-well plates under the conditions described above. The medium was aspirated, washed with PBS, and then treated, in duplicate, with 0.1 mL of the medium containing different concentrations of **NJ1060** NPs (0-400 μg/mL). Staurosporine (STS, 200 nM) was used as a positive control. After a total treatment time for 24 h, proliferation was assayed using the XTT colorimetric cell proliferation kit (Roche), following manufacturer guidelines

10. Animal handling

All mice were purchased from Jiangsu KeyGEN BioTECH Corp., Ltd. and used according to the guidelines of the Laboratory Animal Center of Jiangsu KeyGEN BioTECH Corp., Ltd. Two groups of mice were generated by intravenously injecting **ICG** (200 μL, 2.0 mg/mL) and **IR1061** (200 μL, 2.0 mg/mL), respectively, as control; another group was generated by intravenously injecting **NJ1060** NPs (200 μL, 2.0 mg/mL). And then, three groups were fluorescence imaging for the right hind leg and brain, respectively. The animals with tumors (4t1) were also used for experiments. The animal was generated by intravenously injecting **NJ1060** NPs (200 μL, 2.0 mg/mL) and it was taken for fluorescence imaging for different times (1, 3, 6 ,12 and 24 h) to observe the fluorescence of the tumor position.

11. NIR-II imaging

The real-time in vivo NIR-II Imaging was performed at intravenous injection by using a home built NIR-II spectroscopy set-up in the 900-1500 nm region. The excitation wavelength was an 808 nm semiconductor laser at 200 mW output of power. Excitation at 808 nm was deliberately used to balance absorption and scattering to obtain maximum penetration depth of excitation light for in vivo imaging. Emissions were acquired in the transmission geometry with a 975 nm long pass filter (ScmRock) to prevent the excitation light. The emitted fluorescence from the sample was directed into a spectrometer (Acton SP2300i) equipped with an InGaAs linear array detector (Princeton OMA-V).

Table S1. Chemical structures and photophysical properties of reported NIR-II small molecule dyes from literatures.

Types	NIR-II dyes	Chemical structure
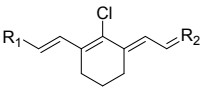	**IR1048**[1]	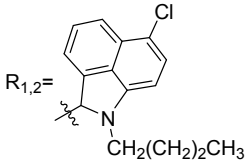 Em=1048 and Φ_f%=0.4 in DCM
	IR1061[1]	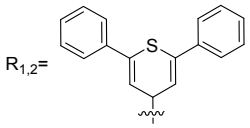 Em=1061 and Φ_f%=1.7 in DCM
	IR1026[2]	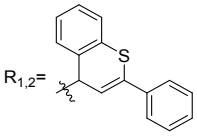 Em=1026 and Φ_f%=0.5 in DCM
	FD-1080[3]	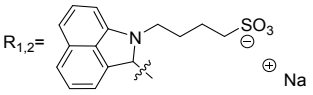 Em=1048 and Φ_f%=0.4 in H_2O
	IR 1100[2]	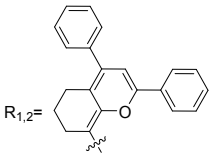 Em=1100 and Φ_f%=N in DCM
	IR 26[4]	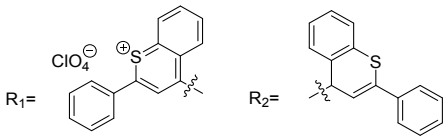 Em=1130 and Φ_f%=0.1 in DCE
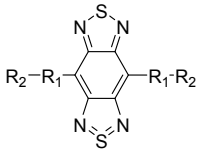	**IR-FGP**[5]	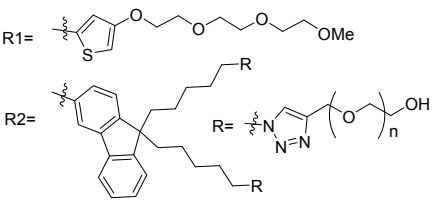 Em=1045 and Φ_f%=1.91 in H_2O
	CH1055[6]	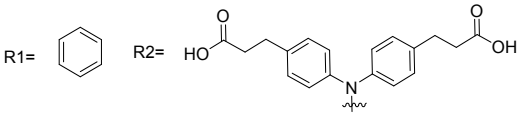 Em=1055 and Φ_f%=0.3 in H_2O

	SCH1100[7]	R1=  R2= 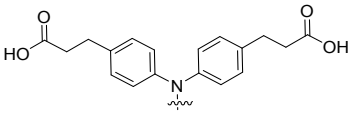 Em=1100 and Φ_f%=N in DCM

Table S2. Calculated electronic excitation energies, oscillator strengths, and related wave functions.

Dye	State[a]	TDDFT//B3LYP/6-31G(d)				
		Energy[eV]	λ[nm]	f[d]	Orbitals (coefficient)[e]	CI[f]
NJ960	$S_0 \rightarrow S_1$[b]	1.6043	773	0.5256	H–L	0.69750
					H-2–L	-0.13999
	$S_0 \rightarrow S_2$	1.9345	641	0.6882	H-1–L	0.70468
	$S_1 \rightarrow S_0$	1.3624	910	0.7328	H–L	0.70727
	$S_0 \rightarrow S_1$[c]	1.6351	758	0.4831	H–L	0.69455
					H-2–L	-0.15676
	$S_0 \rightarrow S_2$	1.9577	633	0.6383	H-1–L	0.70452
	$S_1 \rightarrow S_0$	1.3631	909	0.7324	H–L	0.70726
NJ1030	$S_0 \rightarrow S_1$[b]	1.5578	796	0.4989	H–L	0.70112
					H-2–L	-0.12156
	$S_0 \rightarrow S_2$	1.9189	646	0.6726	H-1–L	0.70439
	$S_1 \rightarrow S_0$	1.4149	876	0.7157	H–L	0.70681
	$S_0 \rightarrow S_1$[c]	1.5874	781	0.4583	H–L	0.69901 -
					H-2–L	0.13646
	$S_0 \rightarrow S_2$	1.9422	638	0.6212	H-1–L	0.70415
	$S_1 \rightarrow S_0$	1.4157	875	0.7152	H–L	0.70680
NJ1060	$S_0 \rightarrow S_1$[b]	1.5060	823	0.5070	H–L	0.70596
	$S_0 \rightarrow S_2$	1.8622	666	0.6920	H-1–L	0.70495
	$S_1 \rightarrow S_0$	1.2654	980	0.7298	H–L	0.70927
	$S_0 \rightarrow S_1$[c]	1.5371	806	0.4688	H–L	0.70494
					H-2–L	0.11000
	$S_0 \rightarrow S_2$	1.8873	656	0.6386	H-1–L	0.70479
	$S_1 \rightarrow S_0$	1.2662	979	0.7289	H–L	-0.70926

[a] Only selected excited state were considered. [b] Water was employed as the solvent for the DFT calculations. [c] Water containing 20% DMSO (v:v) was employed as the solvent for the DFT calculations. [d] Oscillator strength. [e] MOs involved in the transitions. H = HOMO; L = LUMO. [f] Coefficient of the wavefunction for each excitations. The CI coefficients are in absolute values.

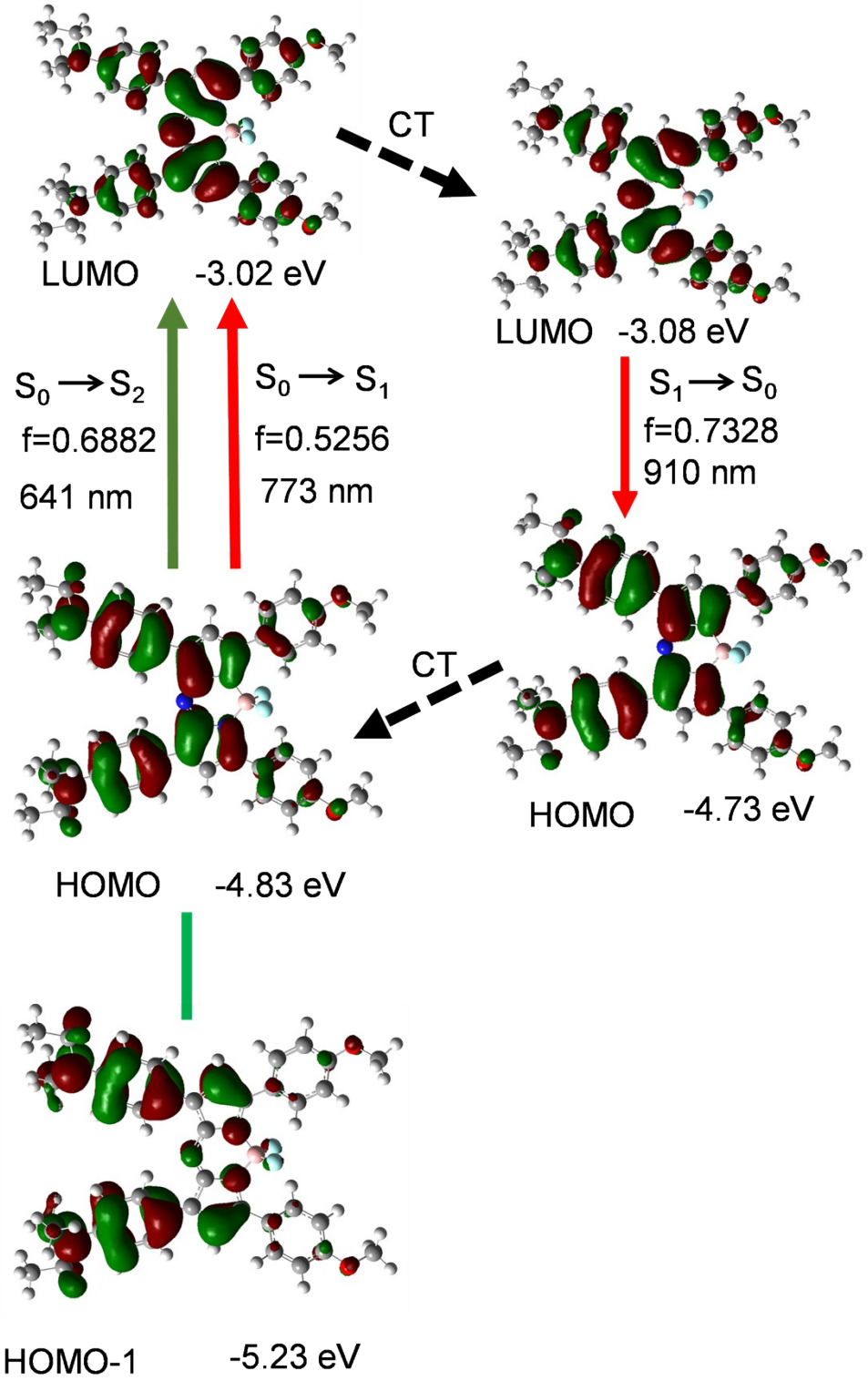

Figure S1. The frontier molecular orbitals (MOs) involved in the vertical excitation (UV-vis absorption) and emission of **NJ960**. Water was employed as the solvent for the DFT calculations. The vertical excitation related calculations are based on the optimized ground state geometry (S_0 state), the emission related calculations were based on the optimized excited state (S_1 state), at the B3LYP/6-31G(d)/level using Gaussian 09W. CT stands for conformation transformation. Excitation and radiative processes are marked as solid lines and the non-radiative processes are marked by dotted lines.

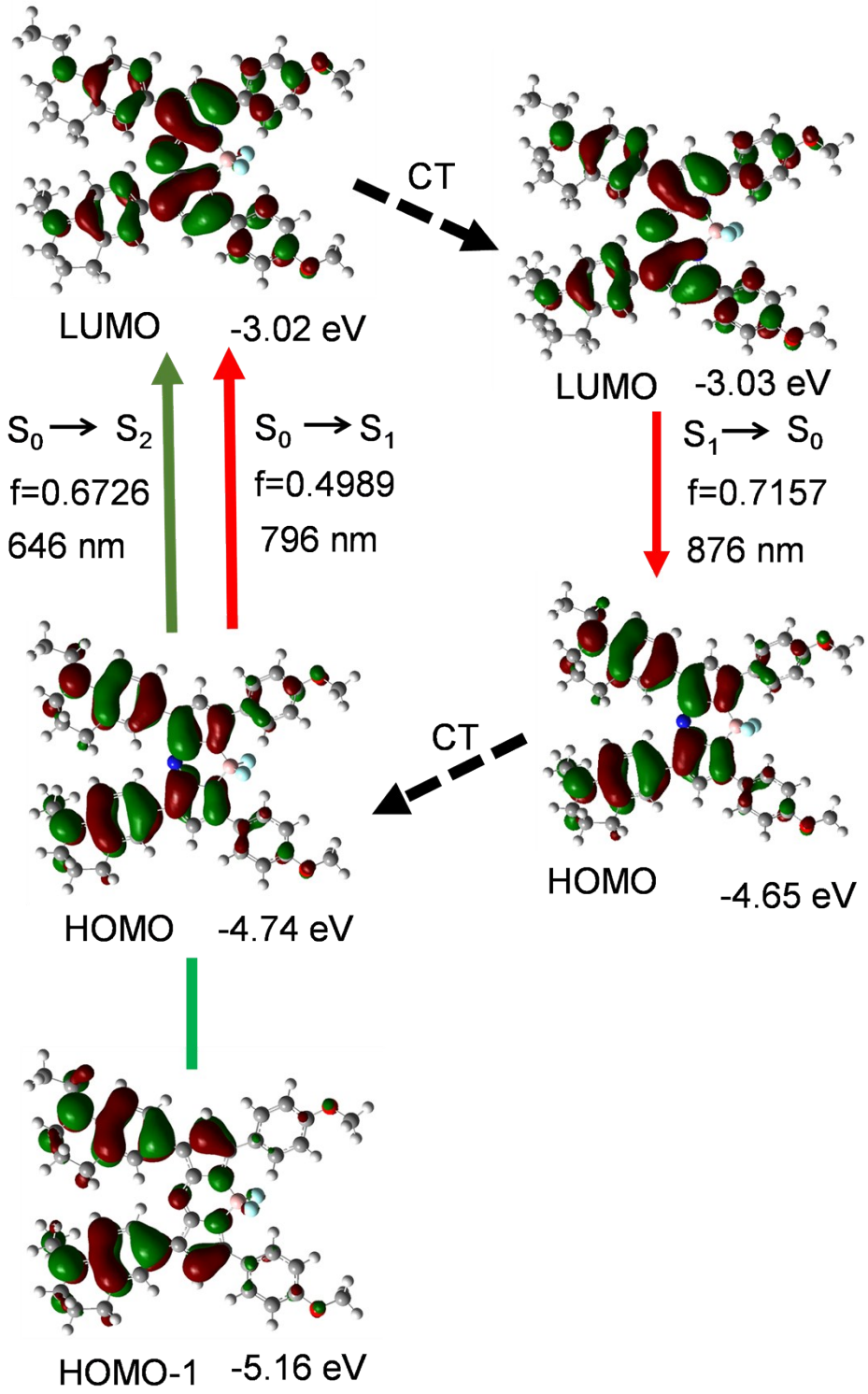

Figure S2. The frontier molecular orbitals (MOs) involved in the vertical excitation (UV-vis absorption) and emission of **NJ1030**. Water was employed as the solvent for the DFT calculations. The vertical excitation related calculations are based on the optimized ground state geometry (S_0 state), the emission related calculations were based on the optimized excited state (S_1 state), at the B3LYP/6-31G(d)/level using Gaussian 09W. CT stands for conformation transformation. Excitation and radiative processes are marked as solid lines and the non-radiative processes are marked by dotted lines.

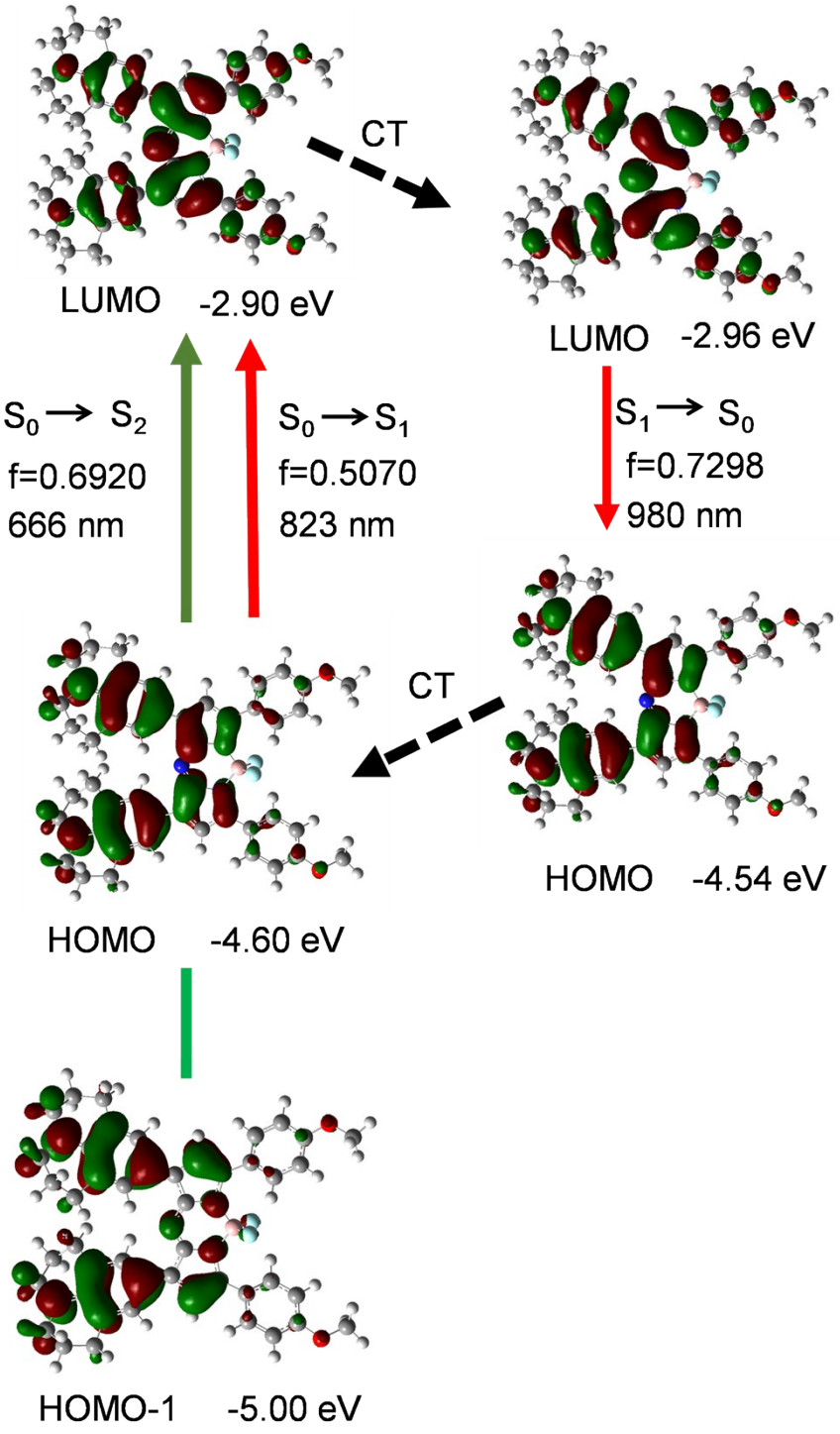

Figure S3. The frontier molecular orbitals (MOs) involved in the vertical excitation (UV-vis absorption) and emission of **NJ1060**. Water was employed as the solvent for the DFT calculations. The vertical excitation related calculations are based on the optimized ground state geometry (S_0 state), the emission related calculations were based on the optimized excited state (S_1 state), at the B3LYP/6-31G(d)/level using Gaussian 09W. CT stands for conformation transformation. Excitation and radiative processes are marked as solid lines and the non-radiative processes are marked by dotted lines.

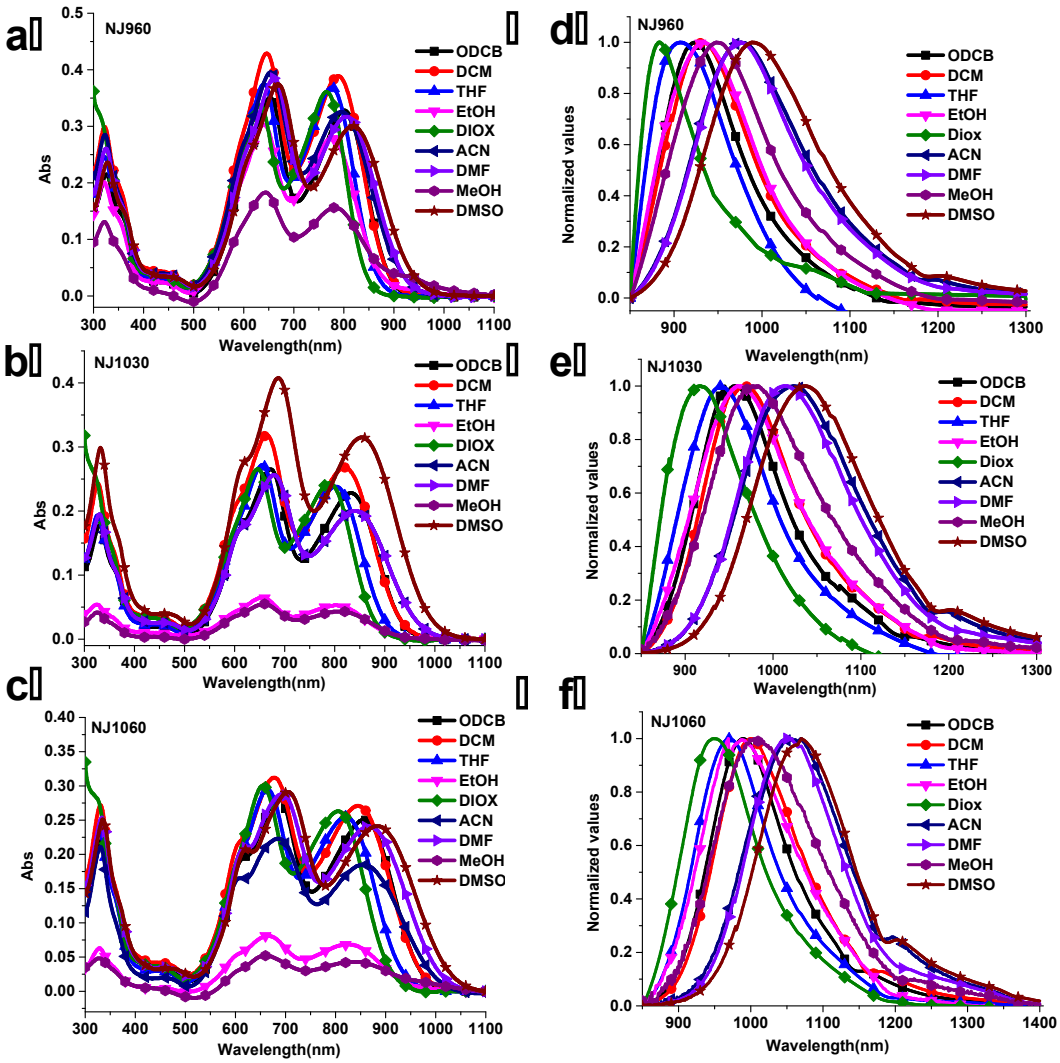

Figure S4. The UV-Vis absorption spectra (a, b, c) and normalized fluorescence spectra (d, e, f) of **NJ960** (5 μM), **NJ1030** (5 μM) and **NJ1060** (5 μM) in various organic solvents (ODCB: 1,2-Dichlorobenzene, DCM: dichloromethane, THF: Tetrahydrofuran, EtOH: Ethanol, DIOX: 1,4-Dioxane, ACN: Acetonitrile, DMF: N,N-Dimethylformamide, MeOH: Methanol, DMSO: Dimethyl sulfoxide). The excitation wavelength is at 808 nm.

Table S3. The photophysical characterization of **NJ960**, **NJ1030**, **NJ1060** in various organic solvents .

Compound	Solvent	$\lambda_{abs(max)}$ (nm)	ε ($cm^{-1}\cdot M^{-1}$)	λ_{em} (nm)	Stokes shift/nm
	ODCB	804	689000	924	123
	DCM	788	817000	933	145
	THF	776	775000	907	131
	EtOH	776	586000	933	157
NJ960	DIOX	765	758000	883	118
	ACN	801	327000	976	180
	DMF	796	665000	976	172
	MeOH	781	327000	948	167
	DMSO	818	630000	989	171
	ODCB	832	495000	956	124
	DCM	820	582000	968	148
	THF	802	517000	941	139
	EtOH	802	115000	963	161
NJ1030	DIOX	786	528000	918	132
	ACN	839	434000	1023	184
	DMF	839	434000	1012	173
	MeOH	808	93000	978	170
	DMSO	854	684000	1036	182
	ODCB	856	564000	989	133
	DCM	844	608000	1002	158
	THF	820	573000	976	156
	EtOH	825	155000	969	144
NJ1060	DIOX	805	591000	948	143
	ACN	855	415000	1056	201
	DMF	867	541000	1005	138
	MeOH	835	96000	1006	171
	DMSO	883	541000	1070	187

(ODCB: 1,2-Dichlorobenzene, DCM: dichloromethane, THF: Tetrahydrofuran, EtOH: Ethanol, DIOX: 1,4-Dioxane, ACN: Acetonitrile, DMF: N,N-Dimethylformamide, MeOH: Methanol, DMSO: Dimethyl sulfoxide)

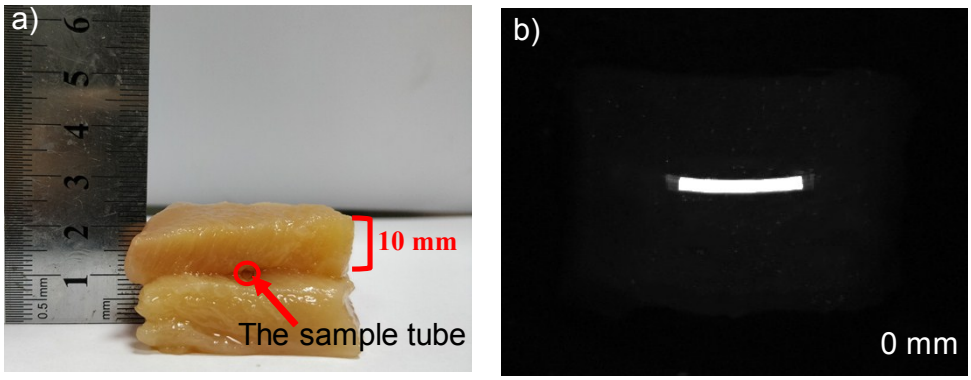

Figure S5. Chicken penetration model assay. (a) A model for the nuggets: the sample tube was covered 10 mm thickness of chicken. (b) The fluorescence image of tube with 0 mm thickness of chicken.

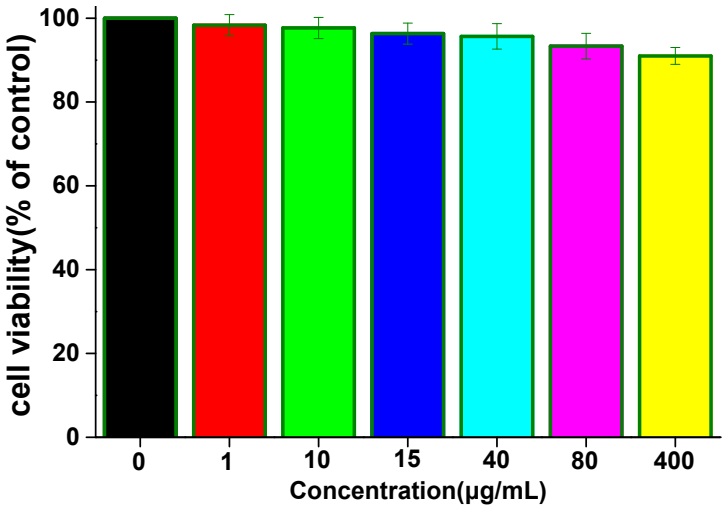

Figure S6. Cytotoxicity of different concentrations of **NJ1060** NPs against HepG2 cells for 24 h.

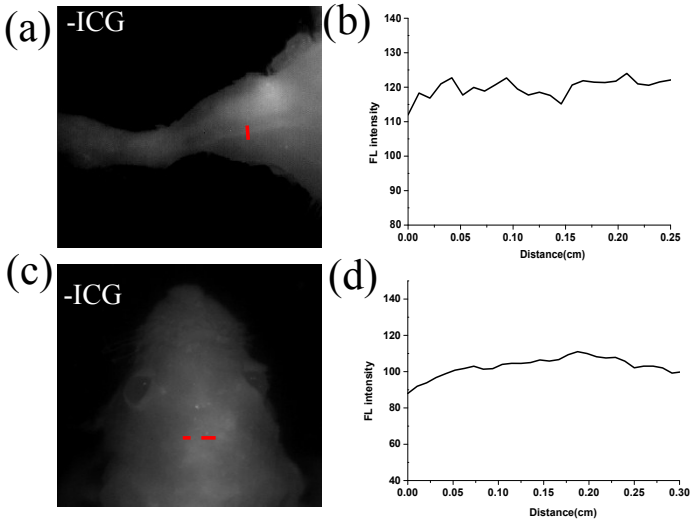

Figure S7. NIR-II images (**ICG**) of the mouse hind limb (a) and brain (c). The emission intensity profiles of a red line of interest in a (b) and c (d).

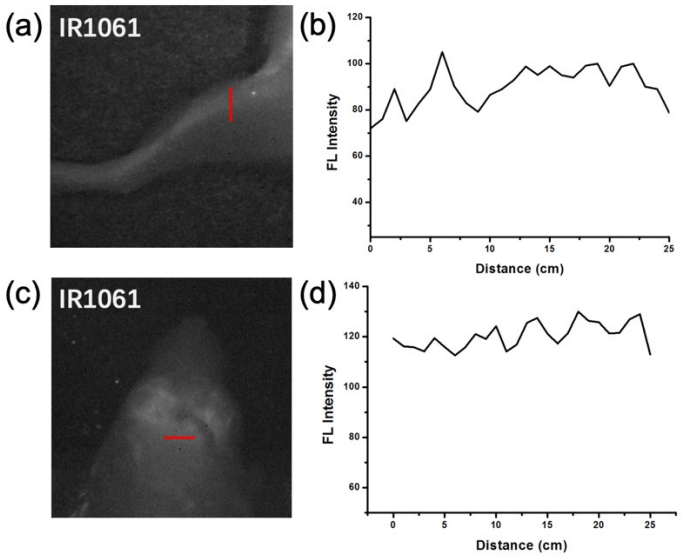

Figure S8. NIR-II images (**IR1061**) of the mouse hind limb (a) and brain (c). The emission intensity profiles of a red line of interest in a (b) and c (d).

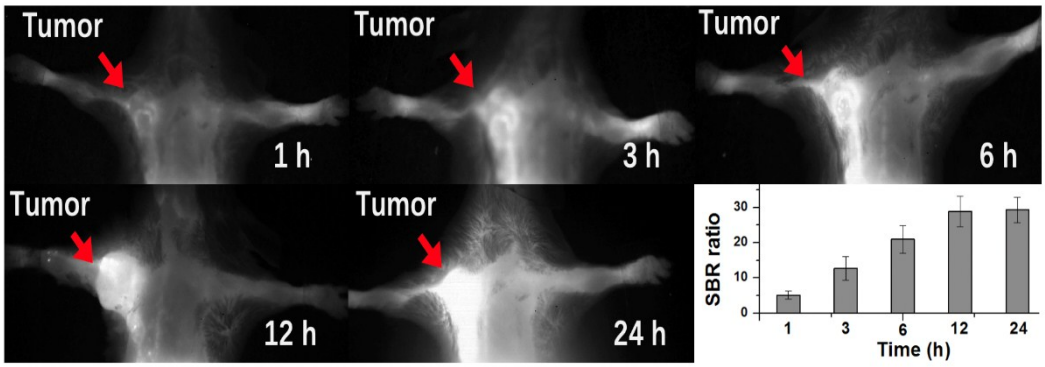

Figure S9: The NIR-II images (IR1061) of the 4T1 tumor at different time points after tail-vein injection of **NJ1060** NPs under an 808 nm laser excitation and SBR ratios of the tumor at different time.

12. ^{1}H, ^{13}C-NMR and HRMS Spectra.

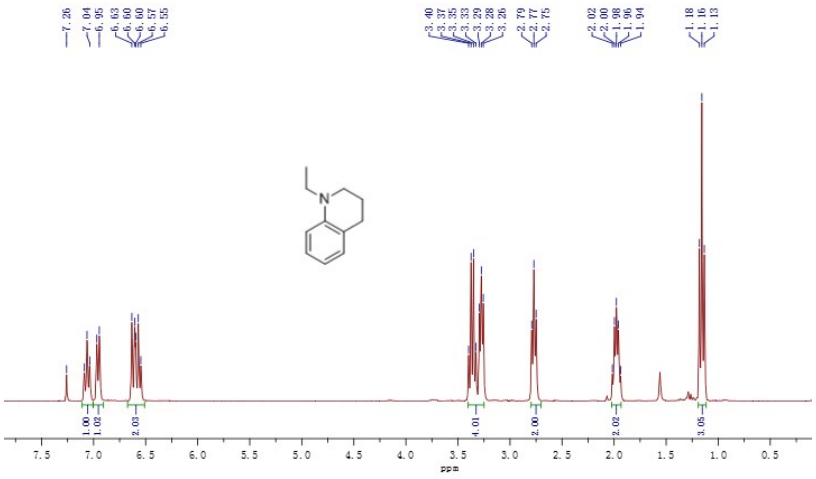

^{1}H NMR spectrum of **1**

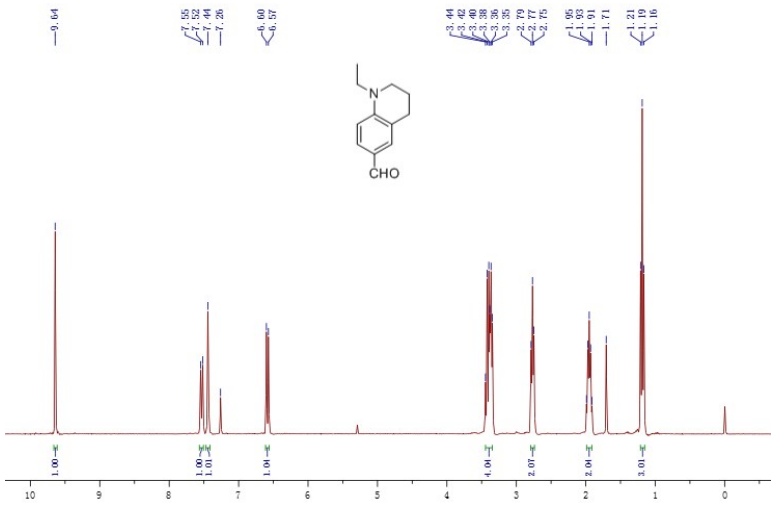

^{1}H NMR spectrum of **2b**

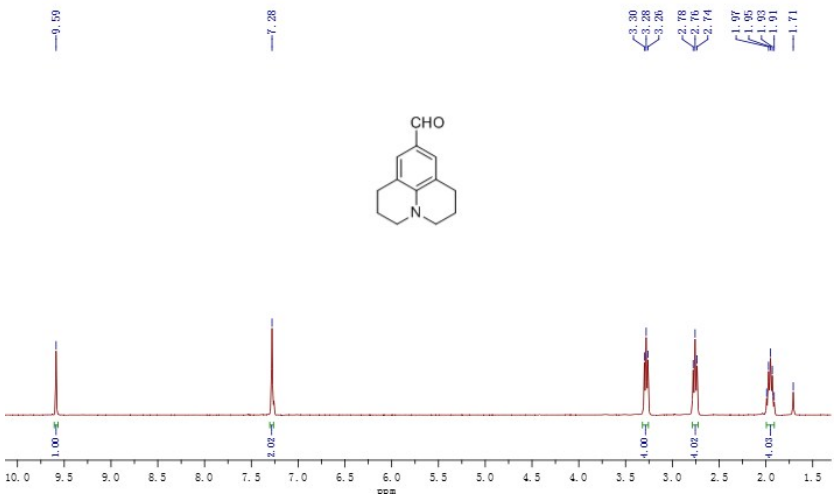

^{1}H NMR spectrum of **2c**

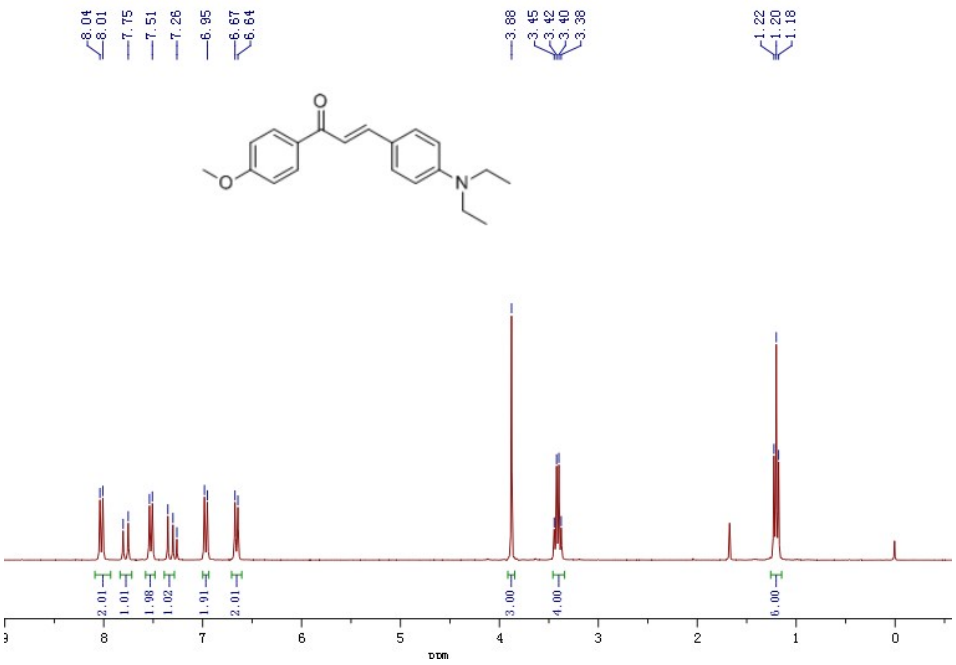

^{1}H NMR spectrum of **3a**

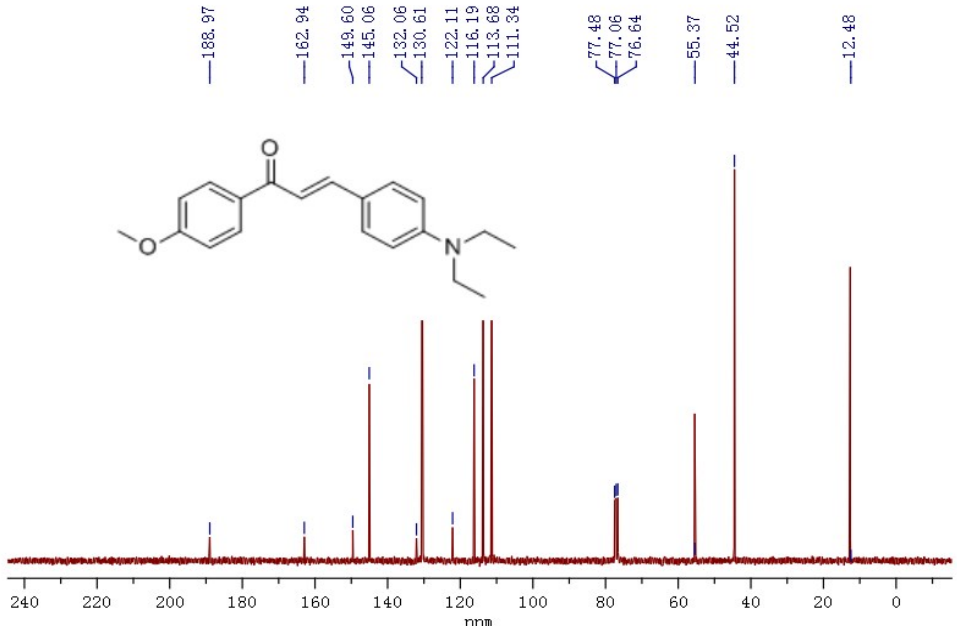

^{13}C NMR spectrum of **3a**

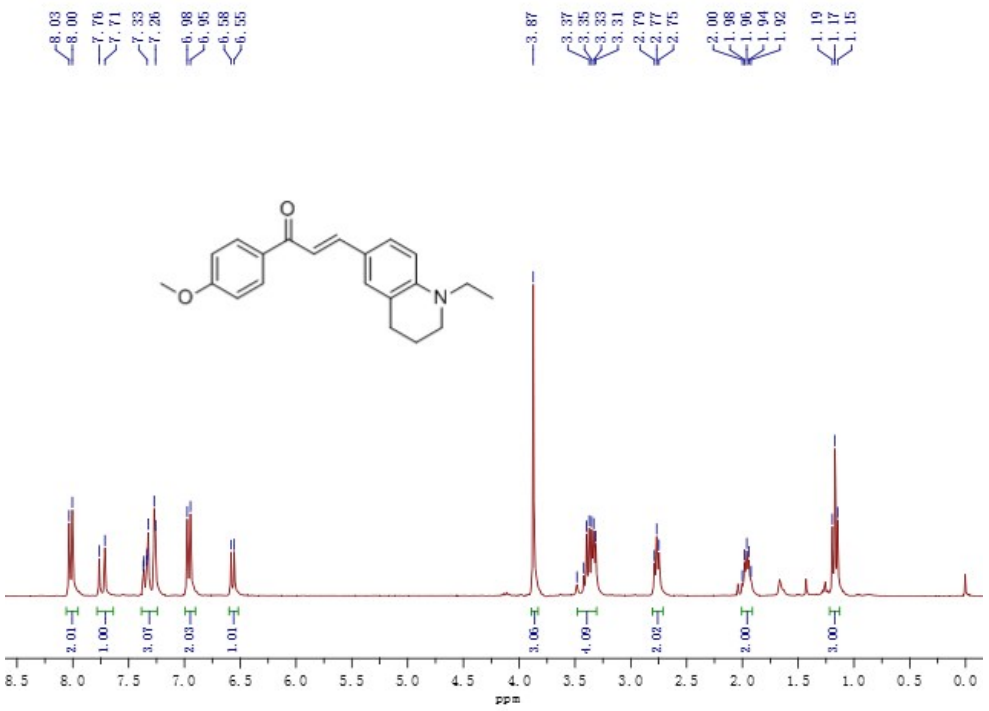

^{1}H NMR spectrum of **3b**

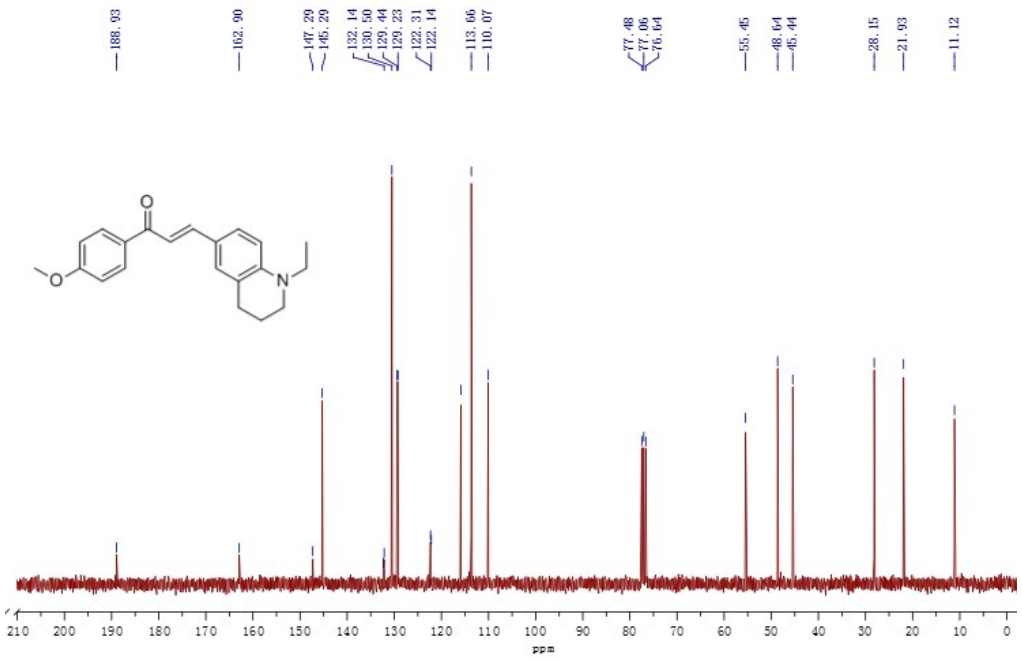

^{13}C NMR spectrum of **3b**

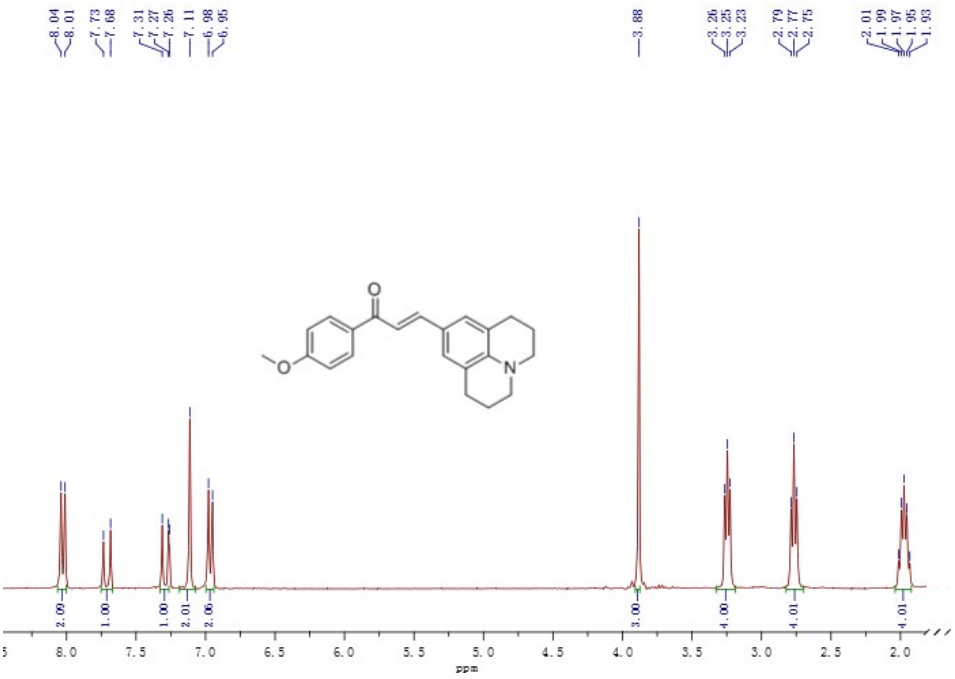

^{1}H NMR spectrum of **3c**

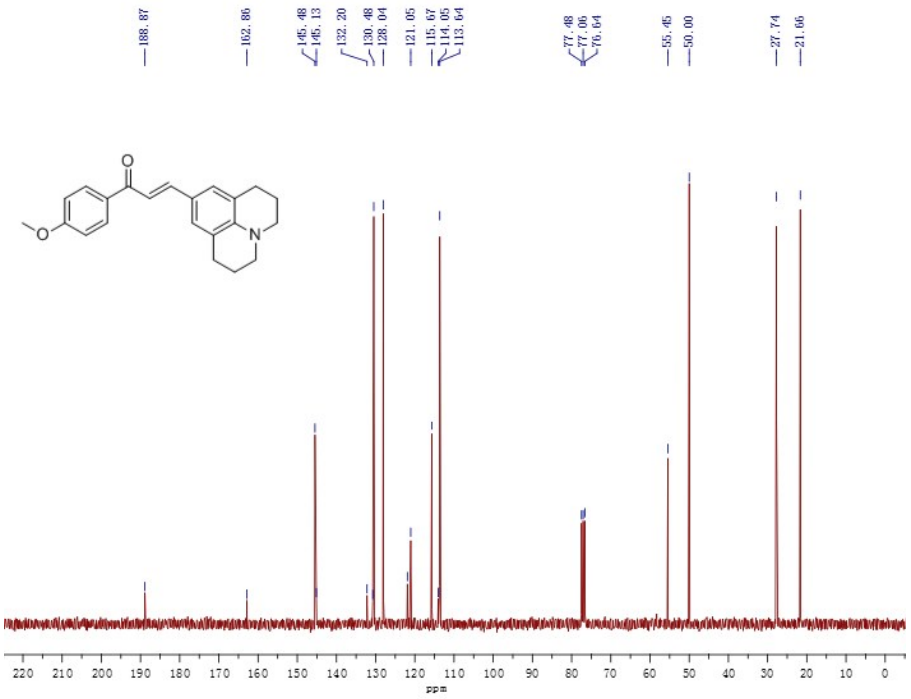

^{13}C NMR spectrum of **3c**

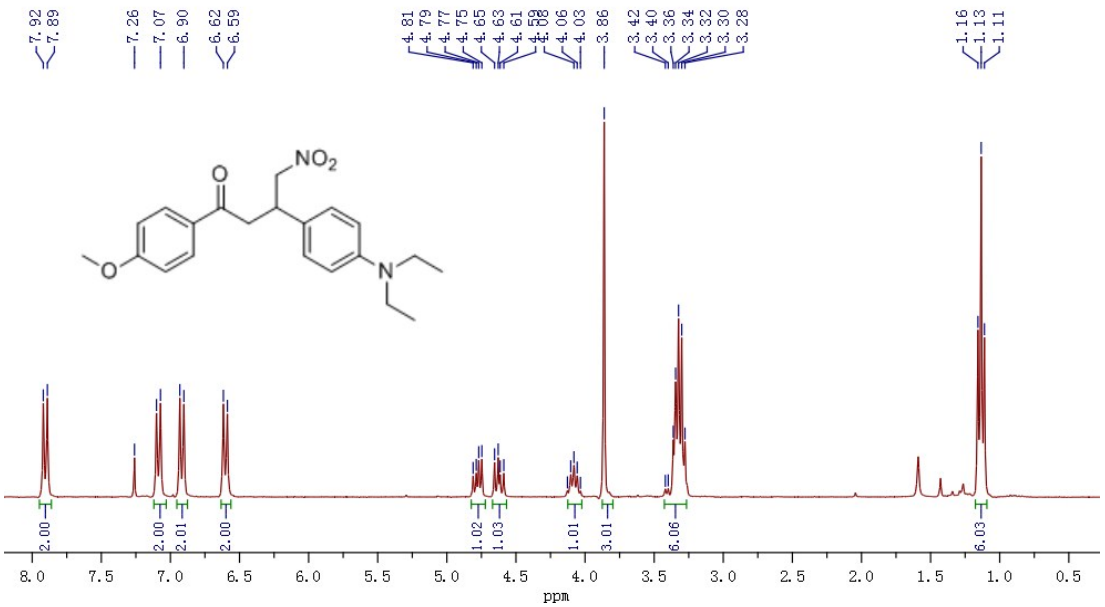

^{1}H NMR spectrum of **4a**

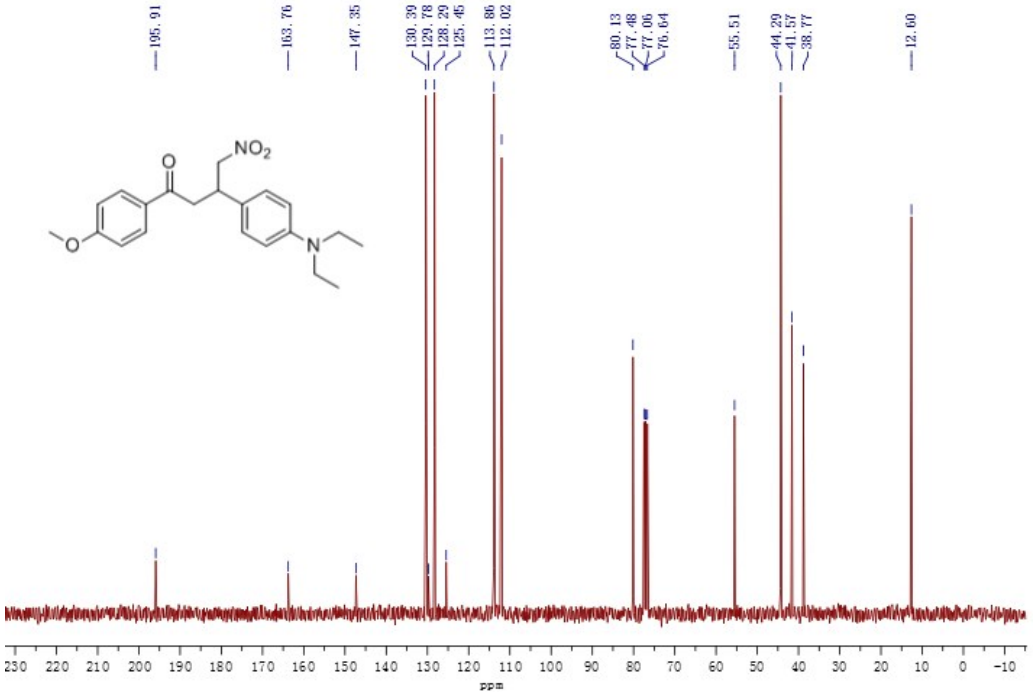

^{13}C NMR spectrum of **4a**

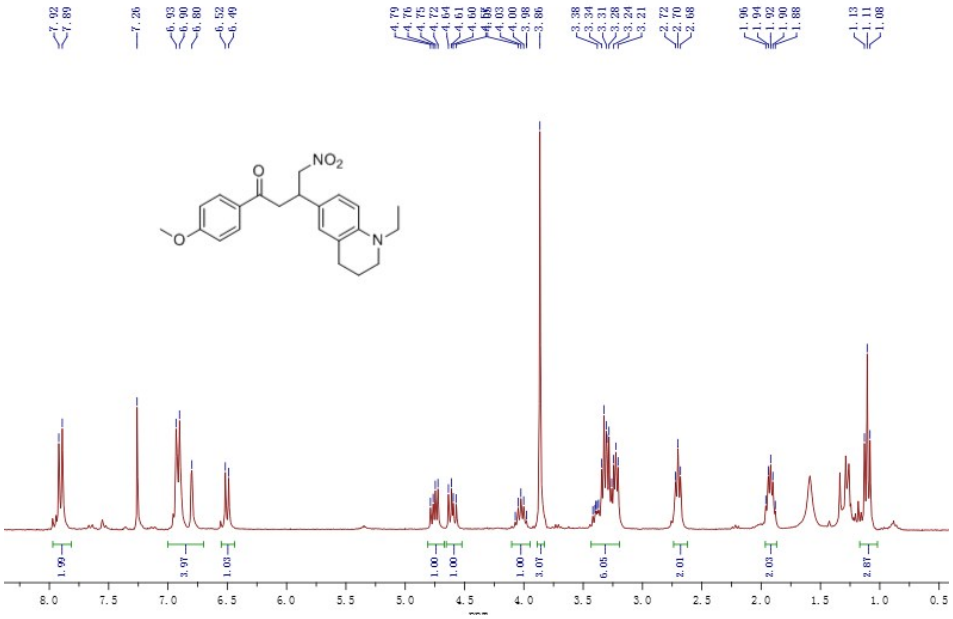

^{1}H NMR spectrum of **4b**

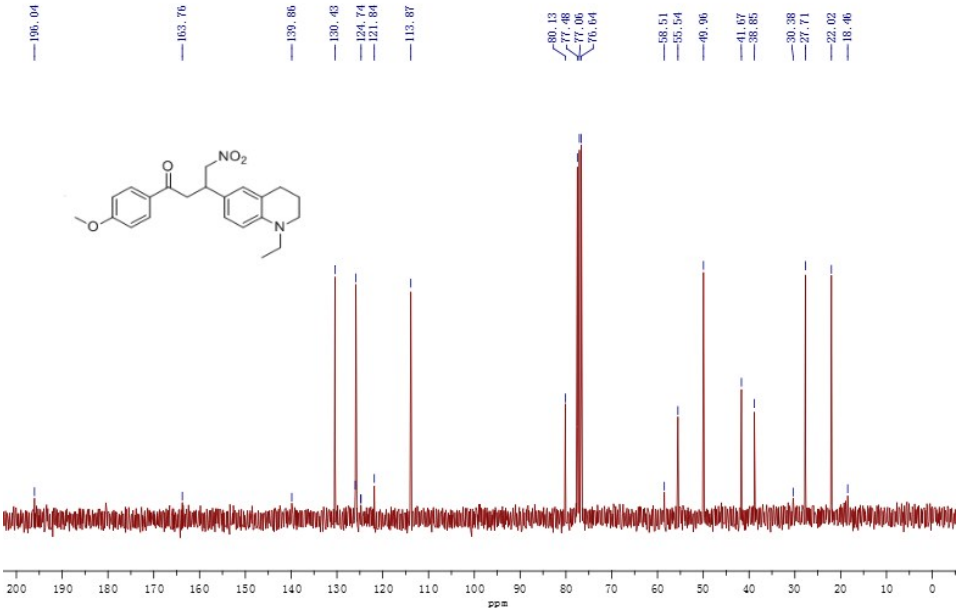

^{13}C NMR spectrum of **4c**

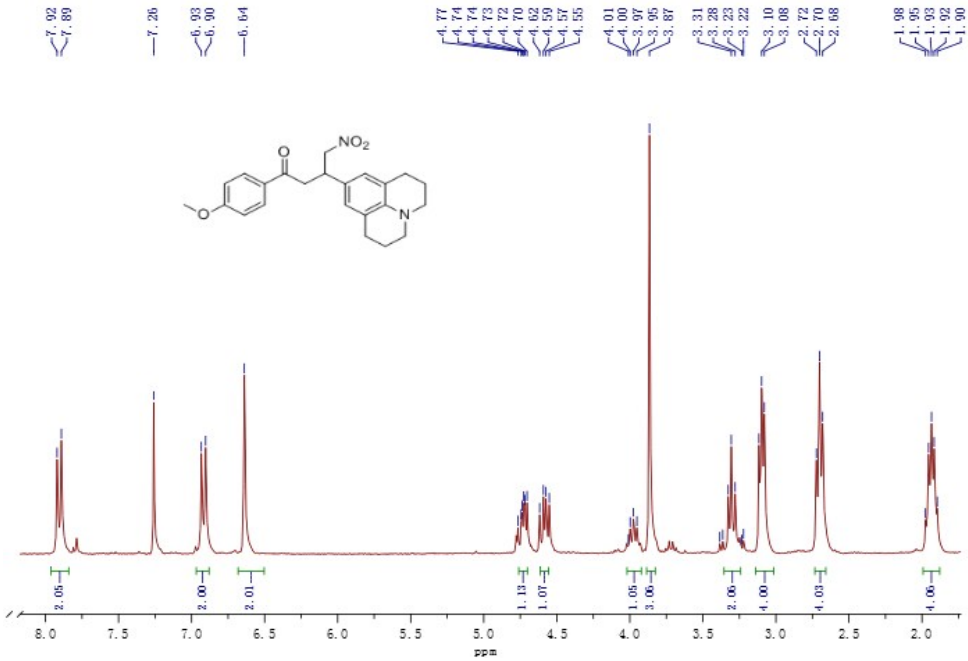

^{1}H NMR spectrum of **4c**

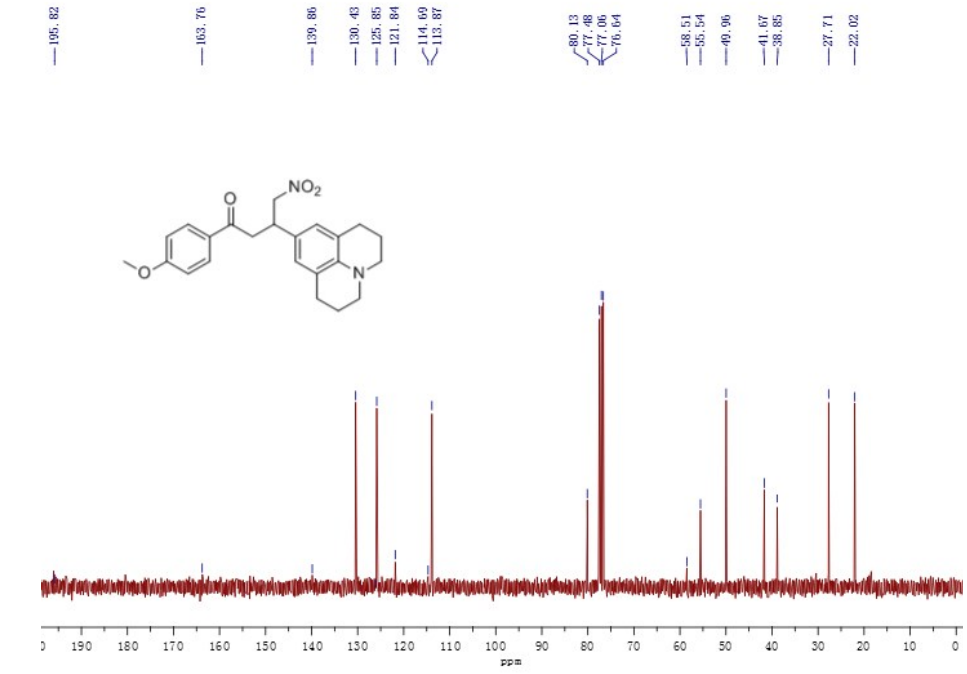

^{13}C NMR spectrum of **4c**

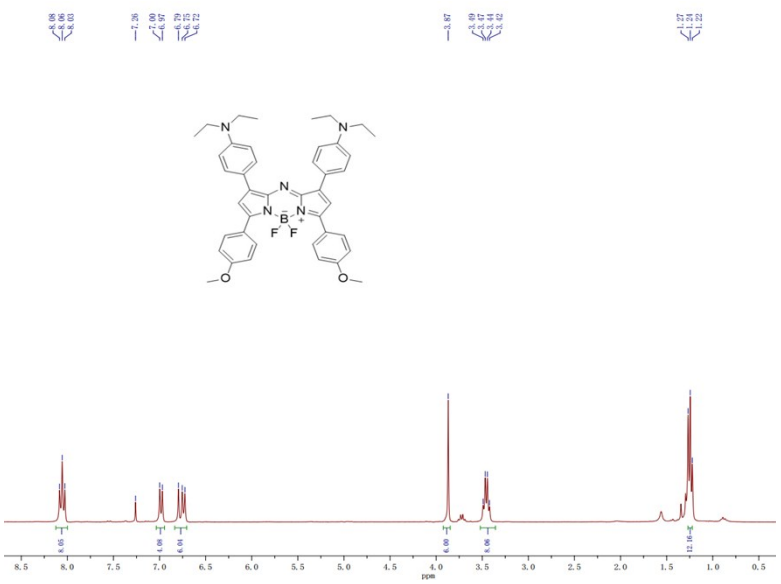

^{1}H NMR spectrum of **NJ960**

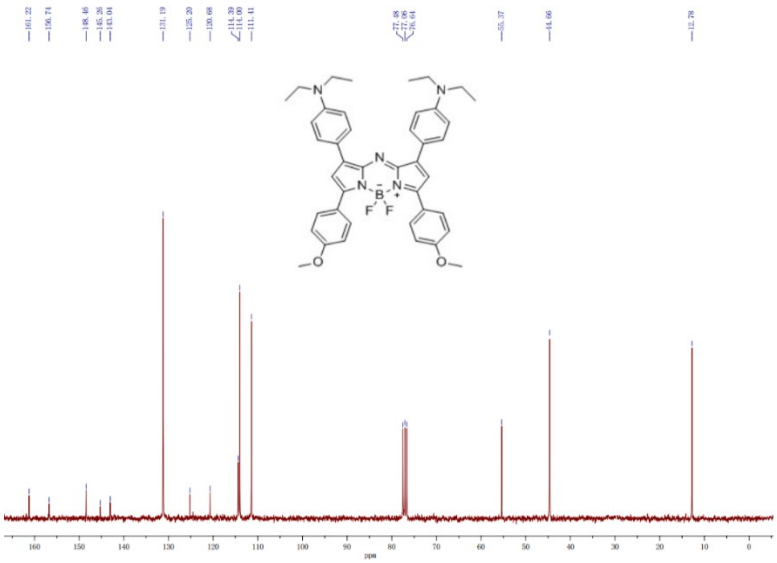

^{13}C NMR spectrum of **NJ960**

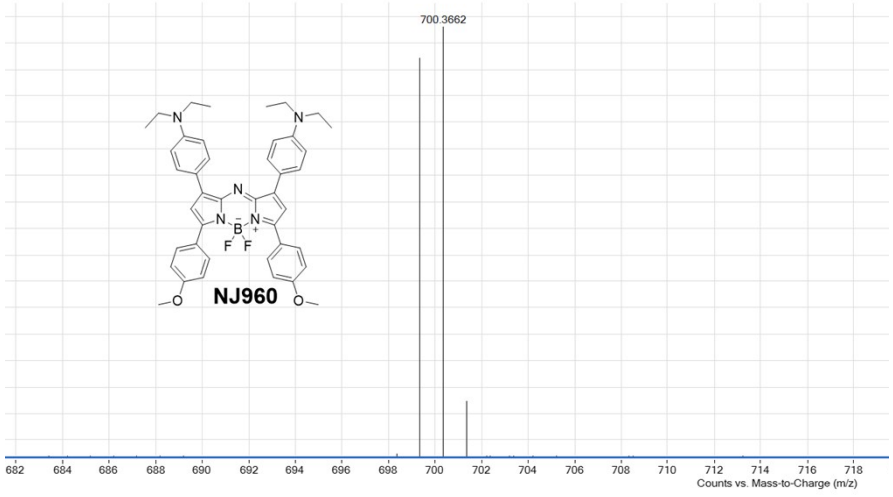

HRMS of **NJ960**

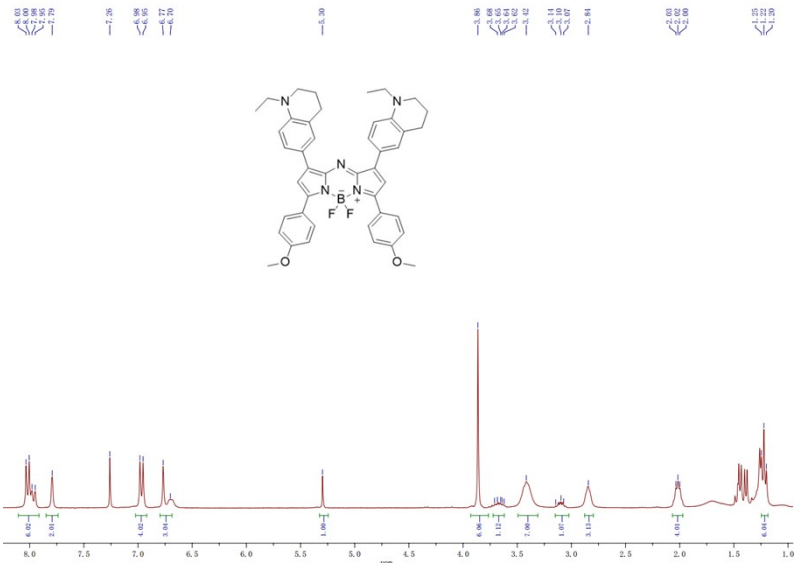

^{1}H NMR spectrum of **NJ1030**

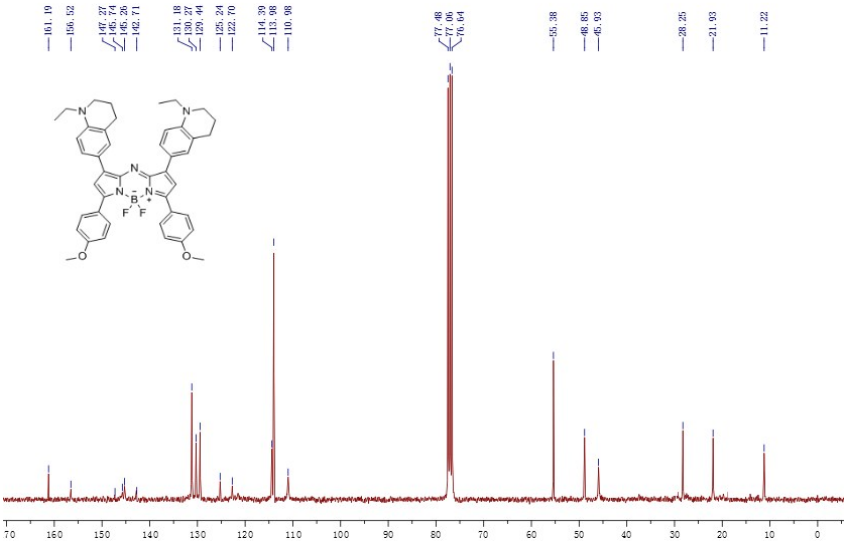

^{13}C NMR spectrum of **NJ1030**

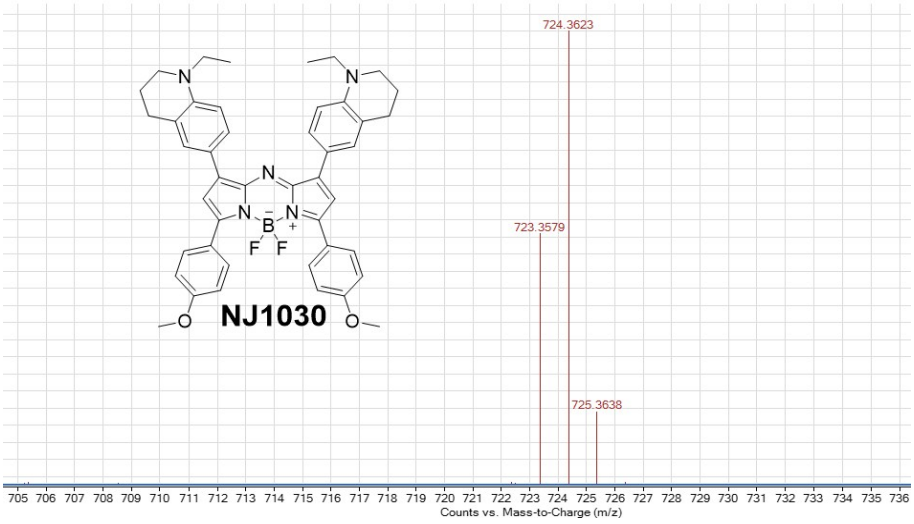

HRMS of **NJ1030**

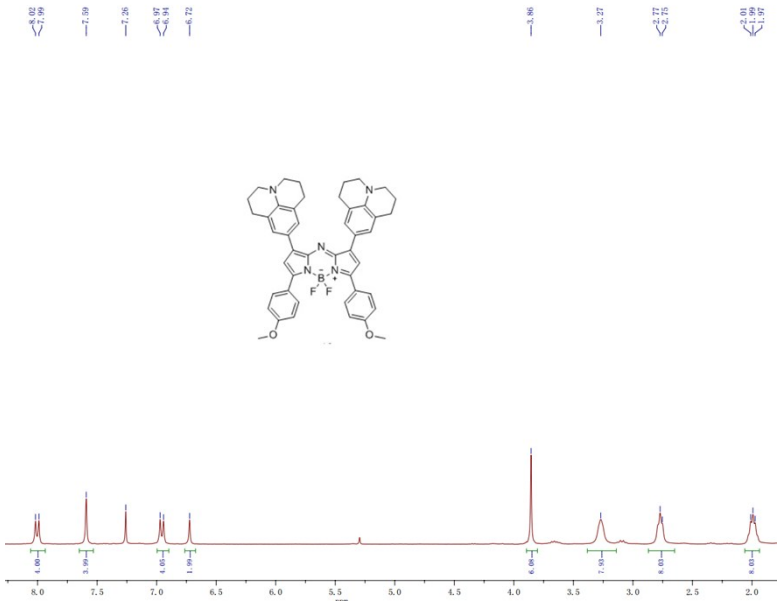

^{1}H NMR spectrum of **NJ1060**.

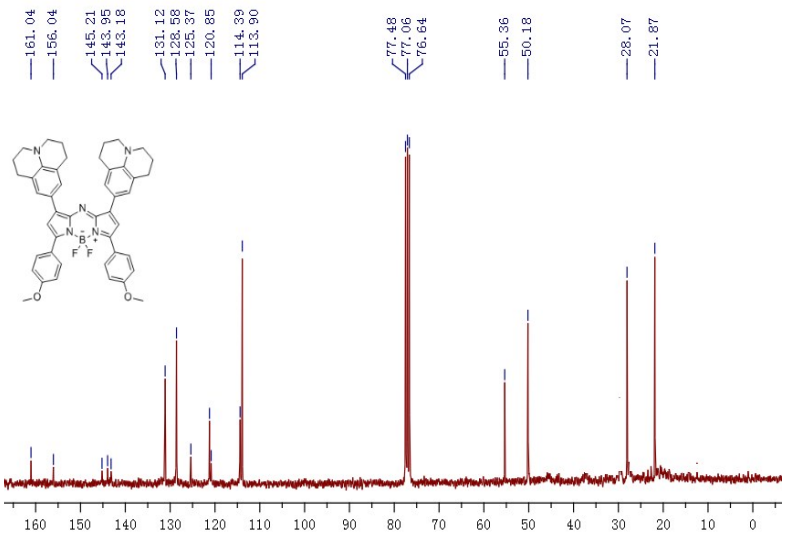

^{13}C NMR spectrum of **NJ1060**

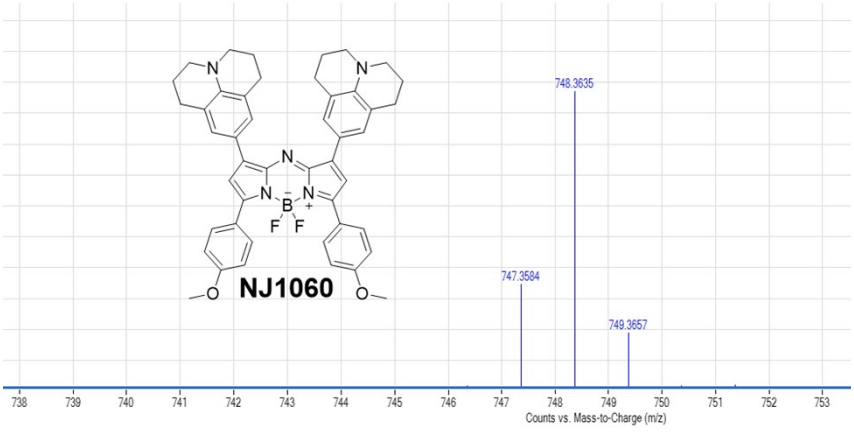

HRMS of **NJ1060**

13. Reference

1 P. Prosposito, M. Casalboni, F. De Matteis, M. Glasbeek, A. Quatela, E. van Veldhoven, H. Zhang. *J. Lumin*. 2001, **94**, 641-644.

2 R. Pizzoferrato, M. Casalboni, F. De Matteis, P. Prosposito. *J. Lumin.* 2000, **87**, 748-750.

3 B. Li, L. Lu, M. Zhao, Z. Lei, F. Zhang, *Angew. Chem. Int. Ed.* 2018, **57**, 7483-7487.

4 S. Hatami, C. Würth, M. Kaiser, S. Leubner, S. Gabriel, L. Bahrig, V. Lesnyak, J. Pauli, N. Gaponik, A. Eychmüller, *Nanoscale* 2015, **7**, 133-143.

5 D. A. Cosco, J. R. Caram, O. T. Bruns, D. Franke, R. A. Day, E. P. Farr, M. G. Bawendi, E. M. Sletten, *Angew. Chem. Int. Ed.* 2017, **56**, 13126-13129.

6 A. L. Antaris, H. Chen, K. Cheng, Y. Sun, G. Hong, C. Qu, S. Diao, Z. Deng, X. Hu, B. Zhang, X. Zhang, O. K. Yaghi, Z. R. Alamparambil, X. Hong, Z. Cheng and H. Dai. *Nat. Mater.* 2016, **15**, 235-242.

7 Y. Sun, Ch. Qu, H. Chen, M. He, Ch. Tang, K. Shou, S. Hong, M. Yang, Y. Jiang, B. Ding, Y. Xiao, L. Xing, X. Hong and Z. Cheng. *Chem. Sci.* 2016, **7**, 6203-6207.